

Makalenin Geliş Tarihi : 25.02.2010
Makalenin Kabul Tarihi : 23.07.2010

EDGE-PRESERVING SUPER-RESOLUTION USING AN ADAPTIVE OUTLIER REJECTION METHOD

Kemal ÖZKAN¹, Erol SEKE²

ABSTRACT : Registration errors are well-known problems in super-resolution restoration applications. Local outliers are caused by the registration errors and objects in motion. Instead of blind rejection of local outliers, we favor for the detected edges. For that, pre-estimated high-resolution image is searched for some specified edge and corner patterns. Outlier rejection is performed based on the pattern found. The method is shown to reduce over-blurring caused by the regularization that is common in iterative super-resolution restoration algorithms.

KEYWORDS : Super-resolution, outlier removal, image restoration

UYARLANABİLİR AYKIRI DEĞER AYIKLAMA YÖNTEMİYLE KENAR KORUMALI YÜKSEK ÇÖZÜNÜRLÜK

ÖZET : İmge çakıştırma hataları yüksek çözünürlük uygulamalarında önemli bir problem oluşturmaktadır. Yerel aykırı değerler sahne içindeki hareketli nesnelere ve çakıştırma hatalarından kaynaklanmaktadır. Bu çalışmada, aykırı değerler bir dayanak olmadan atılmak yerine, resimler içinde belirlenen kenarlar ve köşeler gözönüne alınarak ve bulunan yerel yapıya göre işlem dışında tutulmaktadır. Önerilen yöntemin yinelemeli yüksek çözünürlük algoritmalarında sıklıkla kullanılan düzenleyicilerden doğan aşırı bulanmayı azalttığı deneysel olarak gösterilmiştir.

ANAHTAR KELİMELER : Yüksek çözünürlük, aykırı değer ayıklama, görüntü iyileştirme

¹ Eskişehir Osmangazi Üniversitesi, Mühendislik-Mimarlık Fakültesi, Bilgisayar Mühendisliği Bölümü, 26480 ESKİŞEHİR

² Eskişehir Osmangazi Üniversitesi, Mühendislik-Mimarlık Fakültesi, Elektrik-Elektronik Mühendisliği Bölümü, 26480 ESKİŞEHİR

I. INTRODUCTION

Reconstructing a higher resolution image using multiple images obtained from different views of the same scene has long been an attractive research area. Several techniques and algorithms with well established theoretical support are already in the daily use. The demand for higher quality images continues to feed interest in the related research area that seems to expand due to inevitable usage in HD and 3D imaging.

Multiframe image restoration can be split into two main steps, namely, registration and synthesis, although there are approaches that combine these in one loop [1]. In order to be able to talk about achieving higher resolution (HR), registration parameters must be found in sub-pixel accuracy. HR or higher quality can only be obtained for image areas where additional information is available. Additional information usually comes from other images of the same region. There must be sub-pixel level translations between images or they can only be used to reduce uncorrelated noise. A simplified observation model is illustrated in Fig.1 where geometric transformations for LR images are shown to be different whereas defocus and spatial sampling blurs are common. In practice, one of the LR images is selected as reference according to which the transformation parameters of other images are estimated. In Fig.1, k^{th} $M \times N$ LR image, $Y_k \begin{bmatrix} n \\ n \end{bmatrix}$, is generated by

$$Y_k \begin{bmatrix} n \\ n \end{bmatrix} = H_{\text{sensor}} ** f(H_{\text{common}} ** X_H \downarrow) + N_k \begin{bmatrix} n \\ n \end{bmatrix} \quad (1)$$

where the function $f_k(\cdot)$ represents the geometric transformations on the original image, $**$ is 2D convolution, \downarrow is sampling and N_k is the noise term. H_{common} and H_{sensor} are the blurs caused by the defocus and the photon summation on the sensor cells respectively. Equation-1 is usually simplified to summarize the relation between the desired HR ($rM \times rN$) image and LR images as $Y_k = H_k X + N_k \quad k=1, \dots, K$ where r is the enlargement factor. Here, Y_k is a $MN \times 1$ column matrix constructed from the columns of $Y_k \begin{bmatrix} n \\ n \end{bmatrix}$ image, X is a $r^2 MN \times 1$ similarly constructed matrix from desired HR image pixels and H_k is a $r^2 MN \times r^2 MN$ square matrix representing geometric transformations and blurs. Equations for all LR images can be combined to have one large system as $Y = HX + N$.

One can generate an image with any desired number of pixels from any number and density of input pixels using an interpolation schema like cubic-splines [2].

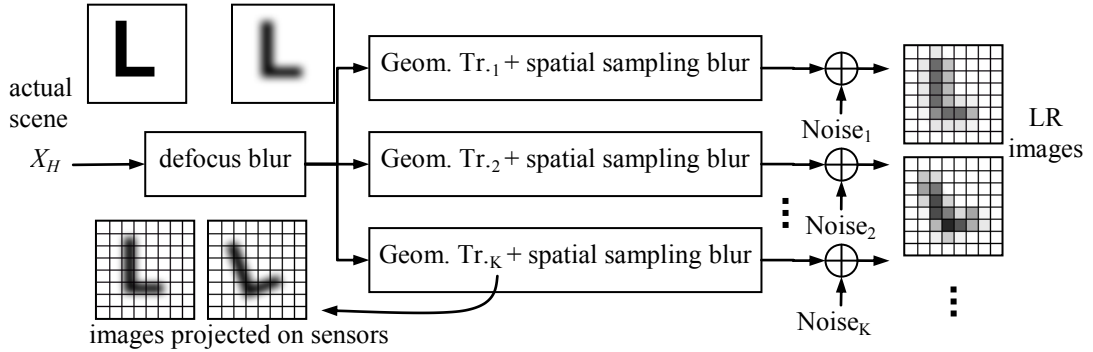


Figure 1. A simplified imaging model. Tr_k 's are rigid rotation and translations.

Restoration of HR images from LR images, however, is not just an increment in the number of pixels. In fact, the term HR should be used to signify more information and higher accuracy in representing the original. This fact is evaluated by Tsai and Huang [3]. They recovered aliased higher frequency components in LR images using the fact that the information contained in LR images is independent. This approach implies that the more aliased components the higher the resolution we can get provided that enough number of independent LR images exist. The motion model used by Irani and Peleg [4] included small rigid rotations. They first estimated an initial HR image from which synthetic-LR images are obtained by employing pre-estimated motion and blur parameters. The difference between synthetic and original LR images is used as a metric to update the parameters, an iterative approach summarized in Fig.2. Forward path in Fig-2 is quite clear, however the methodology implied by 'update estimate' and 'update parameters' makes the difference in terms of final estimate and convergence. One may observe that the iterative approach depicted in Fig.2 is equivalent to the algorithmic iterative minimization implementation of the problem

$$\hat{X} = \underset{X, H}{\text{ArgMin}} \|HX - Y\|_p^p \quad \text{or, in least squares} \quad \hat{X} = \underset{X}{\text{ArgMin}} \|HX - Y\|_2^2 \quad \text{or}$$

$$\hat{X} = \underset{X}{\text{ArgMin}} \|HX - Y\|_2^2 + \beta\lambda(X).$$

Size of the system is a problem and it requires a-priori constraints and/or regularization techniques like

$$\hat{X} = \underset{X}{\text{ArgMin}} \|HX - Y\|_2^2 + \beta\lambda(X) \quad (2)$$

where $\lambda(X)$ is the regularization term which keeps the system stable and is usually composed of pixel-wise differences in images so that they are penalized.

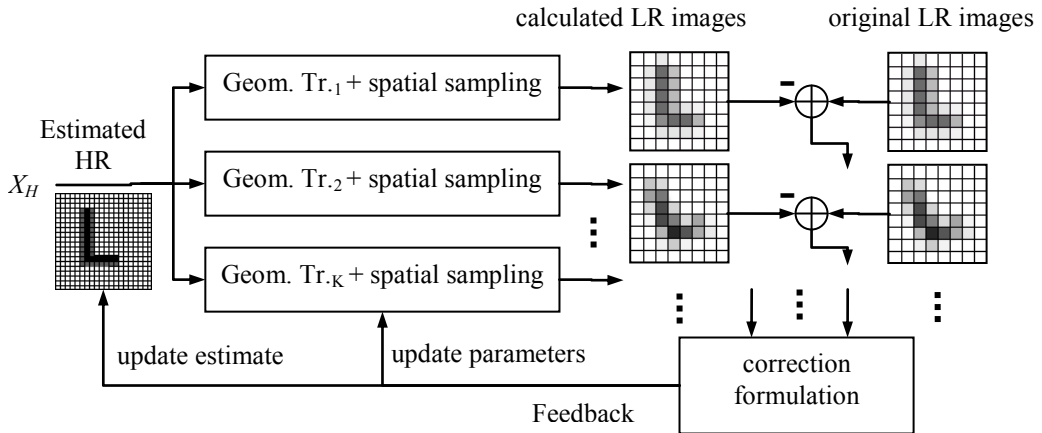


Figure 2. A typical iterative correction algorithm.

Regularization, while preventing instability, causes overly-smoothed SR results. Several researchers attempted to overcome smoothing problem in image restoration algorithms. Hong, Paik, Kim and Lee [5] first prototyped expected edge classes and performed adaptive interpolation accordingly for zooming in images. Battiato, Gallo and Stanco [6] too, employed an edge aware interpolation technique when enlarging images. One of the earliest attempts for deblurring restoration using MAP estimation with generalized Gauss-Markov Random Field

prior has been demonstrated by Bouman and Souer [7]. Method had limited application to super-resolution problems and shortage of efficient algorithms with MAP estimators. Tebaul et al [8] compared some candidate regularization functionals for edge-preserving restoration but offered no method for super-resolution problems. With another single image restoration algorithm, Belge, Kilmer and Miller [9] claimed that discontinuities like edges are detected easily in wavelet domain allowing better adaptation to local features. Existing edge preserving regularization techniques have been summarized and the mathematical foundations of super-resolution are evaluated by Ng and Boze [10]. New approaches like Pan and Reeves' [11], in which MAP estimation technique under Gauss-Markov field assumption and with Huber optimization criterion improved by composing shift variant and shift invariant solutions into one, continue to emerge. The proposed technique is yet to be implemented in super-resolution research, however.

The case of differently blurred noisy samples is studied by Ward [12]. Elad and Feuer [13] have shown that super-resolution restoration is possible when LR images are differently blurred even if there is no relative motion between them. Another iterative algorithm based on projections onto convex sets (POCS) is employed for multiframe restoration by Özkan, Tekalp and Sezan [14], with the claim that the algorithm can easily handle space-varying blur. Later in 1997, Patti, Sezan and Tekalp included the restoration of motion blur using POCS [15]. Elad and Feuer [13], attempted to unify ML and MAP estimators and POCS for super-resolution restoration (SR). Borman and Stevenson [16] and Park, Park and Kang [17] provided comprehensive reviews on SR restoration algorithms and detailed coverage on SR mechanics.

The limits of SR in conventional algorithms are analyzed by Baker and Kanade [18]. They stated that, given the noise characteristics, increasing the number of LR images in an attempt to insert additional information does not limitlessly improve HR image. They suggested a recognition-like technique which they call "hallucination" in order to overcome the limits. Lin and Shum [19] formulated the limits of the reconstruction-based SR algorithms using perturbation theory to and gave the number of LR images to reach that limit without mentioning the preferred SR algorithm. The importance of sub-pixel image registration is obvious as stressed by Baker and Kanade [17] and Lin and Shum [19]. It is widely accepted that accurate estimation of image formation model and its employment in the reconstruction algorithm are

crucial for successful SR implementations. The most valuable contributions to super-resolution research would be the ones that improve subpixel registration accuracy, as proposed by Seke and Özkan [20] where common sensor geometry of array of square sensors has been exploited to refine subpixel registration results.

Assuming that the registration parameters are accurate enough, we, in this paper, also "hallucinate" on what the SR outputs should be and pick LR samples accordingly using a process of outlier rejection. That is, outlier rejection and edge preservation processes are combined in the interpolation phase of an iterative algorithm in an attempt to create an intelligent fusion instead of blind employment of individual techniques. Although the literature on handling the outliers in SR and sub-pixel registration is sparse, it is possible to find some research on methods of determining and rejecting outliers. Trimeche and Yrjänäinen [21], and later Trimeche, Bilcu and Yrjänäinen [22] proposed an adaptive method for excluding image regions where the confidence on the estimated motion parameters is low. Zomet, Rav-Acha and S. Peleg [23] used median estimator in order to avoid outliers. Median estimators may be very effective for visually pleasing outcomes but as argued by Farsiu et al. [24], may prove ineffective for some cases. Legitimacy of median operators in outlier rejection should further be discussed. On the other hand, Farsiu, Robinson, Elad and Milanfar, in another work [25], first calculated bilateral correlations on the fused images, penalized the blocks with low bilateral correlation, and used median estimator and block variances as an outlier removal decision metric.

The situation for synthesis from the registered pixels of LR images is illustrated in Fig-3. The job, here, is to estimate the intensity values at the locations of HR image pixels (shown as small dots) from a number of nearest LR image pixels (example has 3 LR images) which are virtually randomly distributed. It should be kept in mind that for regular images these LR pixels are not point samples but values resulting from the photon summation on the sensor cells with have finite surface areas. Therefore, possibilities for model assumptions and interpolation techniques are unlimited. As the same technique can be used in both forward and feedback path of the system given in Fig.2, one may chose to employ two different interpolation methods in two places.

In a simple approach, HR pixel values would be calculated using a Gaussian interpolation kernel $w_j = \exp(-\text{dist}(P_j, Q_i)^2 / 2\sigma^2) / N_n$ in a weighted sum formulation $p_j = \sum_{i=1}^R q_i w_i$. The function $\text{dist}(\cdot)$ is the distance between HR and LR pixel coordinates denoted by capital letters as opposed to lowercase letters that represent respective pixel values. N_n is a normalization value making w_j s add up to 1. For the smallest applicable σ , operation resembles nearest neighbor pick method. With unnecessarily large σ , distant LR samples become effective, causing over-blurring. One may perform bilinear, bicubic or other interpolation techniques for HR point [26], keeping in mind that selection of any one of them over others has little basis. On the other hand, the question of how to handle outliers caused by the noisy data is still not answered.

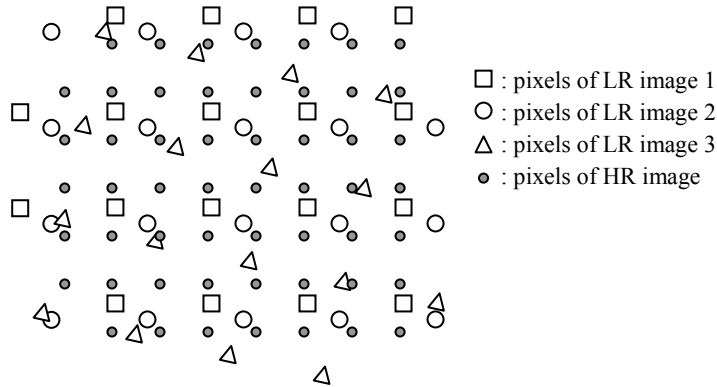


Figure 3. Illustration of LR and HR image pixel locations.

II. EDGES AND OUTLIER HANDLING

In many iterative SR implementations where registration and blur parameters known a priori, HR estimate is updated at each iteration step according to the differences between synthetic and actual LR images for all synthetic-actual LR image pairs using

$$X^{k+1} = X^k + \beta H_{BP}(Y - HX^k) \quad (3)$$

where k is iteration step, H_{BP} is a back propagation matrix (feedback) and β is feedback gain constant dictating the speed of convergence. H_{BP} is initially selected to be the same as forward *point spread function* H without a strong justification. Differences between actual LR images Y and synthetically generated LR images HX^k are penalized. The solution is non-unique and noise, outliers, registration errors, intensity differences, etc. may prevent convergence. Most implementations tend to settle for a blurred solution in order to suppress the effects of noise. It is also difficult to penalize the blur since smoothing an image has little effect on SNR [19]. It is possible, however, to adapt the algorithm in favor of known or detected edge-like features and still sustain convergence.

Use of median operators against outliers are suggested [24, 27] although many researchers claim that median operator is not locally optimal [22] in case of richly textured images with Gaussian noise. In this paper, we propose a method for adaptively handling outliers by first checking the existence of such structures. A draft HR estimate is obtained first by interpolating LR pixel field using simple weighted averaging. A sharp σ of 0.5 is reasonable for the purpose, assigning very low importance to the samples other than very close ones. Initial HR estimate can be generated using any popular fast algorithms like "shift & add" [25]. Resulting HR estimate is searched for the patterns given in Fig.4, and their rotated versions. In Fig.4, the value difference of the darker HR pixel and the center HR pixel is less than a given Δ_b , whereas the values of white areas are higher or lower than this band (Δ_b in our experiments is empirically selected to be 4-5% of the maximum possible intensity in image). Assumption here is that the majority of LR pixels in the vicinity are not outliers; hence do not affect the local pattern. The simple patterns given in Fig-4 cover most of the edges, corners and flat areas. Other possible patterns are not analyzed in our work and simply left as calculated using weighted average.

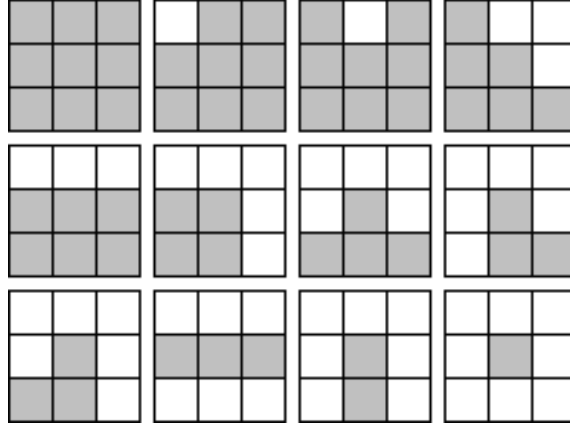


Figure 4. Patterns searched in initial HR estimate.

Once a pattern is detected, the value of HR pixel at the center of the pattern is updated accordingly. For example, in the case of inclined edge as given in fourth pattern in first row of Fig.4, the value of center HR pixel is calculated using only the samples in HR areas within the same band, excluding LR samples within three HR areas located in the upper-right region from the interpolation process altogether. Whether they result from additive noise, spatio-temporal object motion in a series of frames or simply registration errors, LR pixels determined to be outliers within the same band are also penalized using an exponential penalty function. That is, for the example, brighter and darker samples are incorporated into the calculation with lower weight using $b_j = \exp(-|p_i' - q_j|^2 / 2\sigma_b^2) / N_b$. H_{BP} can be separated into two as

$H_{BP} = H_o H_E$ where H_E is calculated once and corresponds to the distance weighted inclusions of LR pixels and H_o is outlier weight matrix updated at every iteration. Values in

H_E can be expressed as
$$h_j = \begin{cases} \exp(-\text{dist}(P_i, Q_j)^2 / 2\sigma_d^2) / N_d & , P_i \in S_j \\ 0 & , \text{otherwise} \end{cases}$$
 for the j^{th} HR

pixel and i^{th} LR sample. S_j is the region which j^{th} HR pixel belongs and is one of the regions shown in Fig-4. Since this value is negligible for distances greater than 3 for the selected σ_d , the iteration Equation 3 is arranged for H_{BP} matrix with 9 columns. The values N_d and N_b

are again normalization values. β is selected to be 0.1 in our experiments giving a reasonable rate of convergence.

III. CASE TESTS

Intuition suggests that an edge-preserving SR algorithm would be most successful on images with full of edges and similar sharp features where other SR algorithms would generate an overly smoothed images. Outlier treatment puts additional pressure on edges. So the test images are selected to have different edginess that we measure using $\eta = \eta_h + \eta_v$, where

$$\eta_h = \frac{1}{M(N-1)} \sum_{r=0}^{M-1} \sum_{c=1}^{N-1} |x_{r,c} - x_{r,c-1}| \quad (4)$$

and

$$\eta_v = \frac{1}{(M-1)N} \sum_{c=0}^{N-1} \sum_{r=1}^{M-1} |x_{r,c} - x_{r-1,c}|, \quad (5)$$

Equation's (4) and (5) are simply average absolute differences between neighboring pixels in horizontal and vertical directions respectively.

LR test images are generated from HR versions by applying different translations and downsampling by at least 5 so that continuous light-field is closely simulated. Five LR image sets, each consisting of 30 translated images, are generated using the sub-pixel translations given in Table 1 and 2. Similar sets are formed using inexact translation parameters and/or with AWG noise of 40dB. As translation-only parameters suffice for the purpose, no other geometric transformation is applied.

Table 1. Translations assigned per LR image set

Img	d_x	d_y	Img	d_x	d_y	Img	d_x	d_y
1	0.00	0.00	11	0.80	0.35	21	0.85	0.15
2	0.15	0.00	12	0.40	0.00	22	0.45	0.90
3	0.85	0.65	13	0.85	0.40	23	0.80	0.55
4	0.20	0.65	14	0.70	0.75	24	0.45	0.60
5	0.60	0.95	15	0.65	0.75	25	0.45	0.20
6	0.95	0.55	16	0.30	0.90	26	0.45	0.50
7	0.65	0.40	17	0.15	0.80	27	0.40	0.90
8	0.85	0.15	18	0.15	0.35	28	0.90	0.30
9	0.00	0.60	19	0.15	0.60	29	0.00	0.65
10	0.10	0.70	20	0.40	0.70	30	0.25	0.35

Table 2. Translations with added registration errors

LR Imgs	$d_x+\epsilon_x$	$d_y+\epsilon_y$	$d_x+\epsilon_x$	$d_y+\epsilon_y$	$d_x+\epsilon_x$	$d_y+\epsilon_y$
1, 11, 21	0.00000	0.00000	0.86925	0.29681	0.86936	0.06589
2, 12, 22	0.16498	0.00076	0.37073	-0.02726	0.48173	0.99549
3, 13, 23	0.74373	0.63747	0.89446	0.31725	0.74795	0.46805
4, 14, 24	0.14015	0.68229	0.60669	0.70736	0.43699	0.52614
5, 15, 25	0.50802	0.88546	0.69118	0.84030	0.43778	0.24770
6, 16, 26	1.04080	0.48835	0.36186	0.82807	0.51670	0.50873
7, 17, 27	0.60176	0.34086	0.21684	0.75355	0.36899	0.99348
8, 18, 28	0.93621	0.15431	0.18273	0.36945	0.99136	0.32555
9, 19, 29	-0.04158	0.55675	0.09571	0.57037	0.05184	0.61079
10,20,30	0.14718	0.75267	0.47744	0.72241	0.29104	0.36287

LR samples from five test sets with η values of 17.6705 (leaves), 13.6313 (map), 12.4796 (tree), 7.6013 (constr) and 6.2204 (window) are given in Fig-5. PSNR values obtained by 13 different SR algorithms along with the proposed "IBP with edge preservation" algorithm are given in Tables 3, 4 and 5 for the 3. MDSP software kindly provided by Milanfar and Farsiu [28] is used for other 12 algorithms. In order for a fair comparison, exact translations listed in Table 1 and 2 are used for all algorithms. It is clear from PSNR values that the proposed handling of edges and outliers is superior in all test cases. The values in last rows are the improvements achieved by the proposed algorithm over the best PSNR among other methods. It is noticeable that the highest improvements are obtained on image sets with high edginess. As edge processing with predetermined patterns is effective only around edges, possible improvement in flat areas may result from outlier rejection only.



Figure 5. Sub-pixel translated LR test images are obtained from HR counterparts using the translation parameters given in Tables 1 and 2.

Table 3. Resulting PSNRs on images with no added noise

<i>SR Method</i>	<i>leaves</i>	<i>map</i>	<i>tree</i>	<i>constr</i>	<i>window</i>
S&A	27.4843	29.3176	27.2318	29.6035	32.9934
Bilateral S&A	26.7799	28.6017	26.5292	29.2337	32.7251
S&A w, iterative deblurring	26.4158	28.5663	26.5696	28.4146	30.5839
Bilateral S&A w, iter, deblur,	26.6046	28.7296	26.3108	28.6335	30.0819
Median S&A	27.4642	29.3003	27.2147	29.5789	32.9733
Median S&A w, iter, deblur	26.3442	28.3968	26.4323	28.3162	30.3959
Iterative norm 2	29.1334	31.0326	28.6600	30.6516	34.5938
Iterative norm 1	28.1437	29.4875	27.3996	29.5086	33.8005
Norm 2 data with L1 regul,	28.0274	30.3508	27.9121	29.9297	33.9323
Robust L2 regularization	21.0803	-	25.9064	21.9974	14.5059
Robust L1 regularization	26.3006	27.0368	26.1096	29.4958	31.3686
Cubic interpolation	28.1634	29.8024	27.6868	29.8826	33.5038
IBP with edge preservation	30.9299	32.8076	29.9544	31.1369	35.1614
Improvements (see text)	1.7965	1.7750	1.2944	0.4853	0.5676

Table 4. Resulting PSNRs on images with 40dB AWG noise

<i>SR Method</i>	<i>leaves</i>	<i>map</i>	<i>tree</i>	<i>constr</i>	<i>window</i>
S&A	27.4531	29.2572	27.1649	29.5671	32.8326
Bilateral S&A	26.6670	28.5445	26.7272	29.1880	32.2739
S&A w, iterative deblurring	26.3478	28.5455	26.4763	28.3229	30.4712
Bilateral S&A w, iter, deblur,	26.3936	28.7605	26.2327	28.5416	30.3197
Median S&A	27.4341	29.2387	27.1495	29.5468	32.8150
Median S&A w, iter, deblur,	26.3465	28.4909	26.4094	28.2379	30.4831
Iterative norm 2	29.1114	30.9800	28.6061	30.6255	34.4578
Iterative norm 1	28.1041	29.4077	27.2806	29.4383	33.6808
Norm 2 data with L1 regul,	27.9839	30.3001	27.8354	29.9127	33.8428
Robust L2 regularization	21.2941	-	26.2884	22.2083	15.1047
Robust L1 regularization	26.2540	26.9132	25.9799	29.4423	31.1863
Cubic interpolation	28.1183	29.7284	27.5977	29.8390	33.2843
IBP with edge preservation	30.4970	32.3319	29.3952	30.9816	34.9966
Improvements	1.3856	1.3519	0.7891	0.3561	0.5388

Table 5. Resulting PSNRs on images with 40dB noise plus registration errors

<i>SR Method</i>	<i>leaves</i>	<i>map</i>	<i>tree</i>	<i>constr</i>	<i>window</i>
S&A	27.0025	28.8306	26.7937	29.4158	32.5678
Bilateral S&A	26.5748	28.5308	26.5856	29.3175	32.2114
S&A w, iterative deblurring	26.6540	28.4257	26.3054	28.7099	31.2032
Bilateral S&A w, iter deblur,	26.4789	27.9912	26.6839	28.6885	30.8345
Median S&A	26.9773	28.8187	26.7860	29.3994	32.5013
Median S&A w, iter, deblur,	26.6255	28.3702	26.7661	28.6649	31.0066
Iterative norm 2	28.7764	30.6411	28.3306	30.4986	34.2444
Iterative norm 1	27.7669	29.0676	27.0446	29.3509	33.2787
Norm 2 data with L1 regul,	27.4842	30.0023	27.5973	29.8600	33.1889
Robust L2 regularization	21.1054	-	25.5723	22.0551	14.5712
Robust L1 regularization	26.7193	26.6395	26.5259	29.8561	31.9080
Cubic interpolation	27.8888	29.6037	27.4977	29.7817	33.2953
IBP with edge preservation	29.8652	32.0119	29.2363	30.9192	34.9388
Improvements	1.0888	1.3708	0.9057	0.4206	0.6944

In Fig.6, zoomed in sections of the SR images generated by "iterative norm 2" and the proposed method indicate that, although the PSNR values are not very different, sharpness is clearly improved by the latter. Distortions seen on the long horizontal edge in the upper region of the SR images is a sign of registration errors and sub-optimal feedback matrix.

Fig.7 shows SR results for a LR image set (also used by Farsiu et al. [25]) where original high-resolution image is not available. For the fairness count again, the translations calculated by MDSP program is used for "IBP with edge preservation" algorithm too as no actual translations were available. Proposed algorithm managed to improve edges even though the rest of the SR image is almost identical with the best-looking result among other algorithms.



Figure 6. A magnified edge region in **a)** downsampled original. **b)** SR with "iterative norm 2".
c) SR with proposed algorithm (IBP with edge preservation).



Figure 7. a) LR image. b) Iterative norm 2. c) IBP with edge preservation.

IV. CONCLUSION

Limitations of SR algorithms with classical information accumulation approach are pointed out by Baker and Kanade [18] and later by Lin and Shum [19]. Obviously, by gathering more information from more images would help to improve the result within limitations enforced by noise and registration errors. One can make intelligent assumptions during the fusion step and "break the limits", that is, improve the image in both visually and quantitatively. Such an improvement is generally not possible by additional enhancement processes performed on the final images. Denoising algorithms introduce blur whereas sharpening for edge improvement also amplifies noise. By analyzing the local structure, the proposed evaluation method is able to enhance edges and remove outlier samples while retaining detail.

V. REFERENCES

- [1] B. C. Tom and A. K. Katsaggelos, "Reconstruction of a High-Resolution Image by Simultaneous Registration, Restoration, and Interpolation of Low-Resolution Images," Proc. 1995 IEEE International Conf. on Image Processing, pp. II-539-542, Oct. 1995, Washington, DC.
- [2] H.S. Hou, H.C. Andrews, "Cubic splines for image interpolation and digital filtering," IEEE Transactions on Acoustics, Speech, *Signal Processing ASSP-26*, Vol.6, pp. 508–517, 1978.
- [3] R. Y. Tsai and T. S. Huang. "Multiframe image restoration and registration," In R. Y. Tsai and T. S. Huang, editors, *Advances in Computer Vision and Image Processing*, Vol.1, pp. 317–339. JAI Press Inc., 1984.
- [4] M. Irani and S. Peleg, "Improving Resolution by Image Registration," *Computer Vision, Graphics and Image Processing*, vol.53, pp. 231–239, May 1991.
- [5] K.P. Hong, J.K. Paik, H. Ju Kim, C. Ho Lee, "An edge-preserving image interpolation system for a digital camcorder", *IEEE Transactions on Consumer Electronics*, Vol.42, No.3, 1996.
- [6] Battiato S., Gallo G., Stanco F., "A Locally-Adaptive Zooming Algorithm for Digital Images", *Elsevier Image Vision and Computing Journal*, Vol.20, No.11, pp.805-812, 2002.
- [7] C. Bauman, K. Sauer, "A Generalized Gaussian Image Model for Edge-Preserving MAP Estimation", *IEEE Transactions on Image Processing*, Vol.2, No.3, pp.296-310, July 1993.
- [8] S. Teboul, L. Blanc-Féraud, G. Aubert, M. Barlaud, "Variational approach for edge-preserving regularization using coupled PDE's", *IEEE Transactions on Image Processing*, Vol.7, No.3, pp.387-397, 1998.
- [9] M. Belge, M.E. Kilmer, E.L. Miller, "Wavelet domain image restoration with adaptive edge-preserving regularization", *IEEE Transactions on Image Processing*, Vol.9, No.4, pp.597-608, 2000.
- [10] M.K. Ng, N.K. Boze, "Mathematical Analysis of Super-Resolution Methodology", *IEEE Signal Processing Magazine*, Vol.20, No.3, pp. 62-74, 2003.

- [11] R. Pan, S.J. Reeves, "Efficient huber-markov edge-preserving image restoration", *IEEE Transactions on Image Processing*, Vol.5, No.2, pp.3728-3735, 2006.
- [12] R. K. Ward, "Restorations of Differently Blurred Versions of an Image with Measurement Errors in the PSF's", *IEEE Transactions on Image Processing*, Vol.2, No.3, pp.369-381, 1993.
- [13] M. Elad and A. Feuer, "Restoration of a Single Superresolution Image from Several Blurred, Noisy and Undersampled Measured Images", *IEEE Transactions on Image Processing*, Vol.6, No.12, pp.1646-1658, 1997.
- [14] M. K. Özkan, A. M. Tekalp and M. I. Sezan, "POCS Based Restoration of Space-Varying Blurred Images" *IEEE Transactions on Image Processing*, Vol.2, No.4, pp.450-454, 1994.
- [15] A. Patti, M. I. Sezan and A. M. Tekalp, "Superresolution Video Reconstruction with Arbitrary Sampling Lattices and Nonzero Aperture Time", *IEEE Trans. Image Processing*, Vol.6, No.8, pp.1064-1076, 1997.
- [16] S. Borman, R. L. Stevenson, "Spatial Resolution Enhancement of Low-Resolution Image Sequences. A comprehensive Review With Directions for Future Research", Tech. Rep., Laboratory for Image and Signal Analysis, University of Notre Dame, 1998.
- [17] S. C. Park, M. K. Park and M. G. Kang, "Super-Resolution Image Reconstruction: A Technical Overview" *IEEE Signal Processing Magazine*, pp. 21-36, 2003.
- [18] S. Baker and T. Kanade, "Limits on Super-Resolution and How to Break Them", *IEEE Trans. Pattern Analysis and Machine Intelligence*, Vol.24, No.9, pp.1167-1183, 2002.
- [19] Z. Lin and H. Shum, "Fundamental Limits of Reconstruction-Based Superresolution Algorithms under Local Translation", *IEEE Transactions on Pattern Analysis and Machine Intelligence*, Vol.26, No.1, pp.83-97, 2004.
- [20] E. Seke, K. Özkan, "Least Squares Sub-pixel Registration Refinement Using Area Sampler Model", *Journal of Mathematical Imaging and Vision*, Vol.26, No.1-2, pp.19-25, 2006
- [21] M. Trimeche and J. Yrjänäinen, "A Method for Simultaneous Outlier Rejection in Image Super-Resolution", *Lecture Notes in Computer Science*, Vol.2849, No.2003, pp. 188-195, Springer Berlin.
- [22] M. Trimeche, R. C. Bilcu and J. Yrjänäinen, "Adaptive Outlier Rejection in Image Super-resolution", *EURASIP Journal on Applied Signal Processing*, pp.1-12, 2006.

- [23] A. Zomet, A. Rav-Acha, and S. Peleg, “Robust super resolution”, in *Proc. Int. Conf. Computer Vision and Patern Recognition*, vol. 1, pp. 645–650, 2001.
- [24] S. Farsiu, M. D. Robinson, M. Elad and P. Milanfar, “Fast and Robust Multiframe Super Resolution,” *IEEE Transactions on Image Processing*, Vol.13, No.10, pp.1327-1344, 2004.
- [25] Farsiu, S., D. Robinson, M. Elad, P. Milanfar, “Robust Shift-and-Add Approach to Super-resolution”, *Proceedings of the SPIE Annual Meeting*, San Diego, CA, 2003.
- [26] Barber, C. B., D.P. Dobkin, and H.T. Huhdanpaa, “The Quickhull Algorithm for Convex Hulls”, *ACM Transactions on Mathematical Software*, Vol.22, No.4, pp.469-483, 1996.
- [27] M. C. Chiang and T. E. Boulte, “Efficient super-resolution via image warping”, *Image and Vision Computing*, Vol.18, No.10, pp.761–771, 2000.
- [28] S. Farsiu, “MDSP Resolution Enhancement Software – User's Manual”, *University of California, Santa Cruz*, 2004.
- available online: <http://www.soe.ucsc.edu/~milanfar/software/superresolution.html>